

VERTICAL vs. DEVIATED WELLS: BALANCE OF FORCES & EQUATIONS

Victoria Pons
Pons Energy Analytics LLC

ABSTRACT

In sucker rod pumps, accurate downhole data is necessary for control and optimization of wells and assets. Downhole data is calculated from data measured at the surface.

In the 1990s, Sandia National Laboratory was contracted to conduct a series of tests using downhole dynamometer tools on vertical wells. This data validated the use of the wave equation and gave rise to most of the models and programs used today. In today's Oil & Gas world, where a great majority of wells are deviated, operators have difficulty controlling and designing their wells due to inaccurate downhole data and key parameters.

This presentation will focus on comparing the conditions and equations relating to vertical and deviated wells. In a first step, the vertical case will be studied, and the wave equation derived. Challenges to using the wave equation and therefore shortcomings of today's methods will be discussed. In a second step, the deviated case will be explored and compared to the vertical case.

INTRODUCTION

Most likely every well at the end of its life will be artificially lifted using sucker-rod pumping. That represents about 75% of all producing wells in the world.

The concept behind rod pump is simple but it's application can be complicated especially when dealing with today's deviated wellbore. Originally, wells were drilled in a vertical manner. However, progressively this practice has been replaced by drilling wells with complex geometries or long lateral to access shale reservoirs.

In rod pump applications, position and load are measured at the surface, producing what is called a surface dynamometer card. Due to elasticity and friction the work done at the surface is not translated downhole. In order to understand the forces acting on the downhole pump, a downhole dynamometer can be installed but this practice is unreliable, expensive, and unrealistic.

A more realistic approach is to use software analysis to compute downhole data. The most popular of these methods is to solve the one-dimensional wave equation, which models the propagation of stress waves down the rod string at the speed of sound.

The stress waves come from the elastic behavior of the rod string, as is explained [1, 5, 16]. Originally Snyder solved the wave equation using the method of characteristics, see [15], while Gibbs employed separation of variables and Fourier series; see [6, 7, 8, 9]. In 1969, Knapp introduced finite differences to solve the wave equation, which is also the method used by Everitt and Jennings in 1976, see [4, 14]. The Everitt- Jennings method has been implemented and modified by Weatherford International, see [3, 13].

The purpose of this paper is to outline the difference in downhole calculation requirements between vertical and deviated applications of rod pumping.

In a first section, rod pump components and basic pumping concepts are discussed. This section is followed by the derivation of the one-dimensional damped wave equation for the vertical case of the

problem, followed by two examples of available solution methods. Results from the Sandia experiments are discussed in the next section. Next, the balance of forces for the deviated case is presented, followed by two examples of available solution methods. Finally, in a last section, conclusions are presented.

I) Rod Pump Parts and Concept

The work of the prime mover at the surface is reciprocated to a linear motion downhole to lift fluids to the surface and is measured in terms of surface position and load. The horsehead is linked to a tapered rod string which travels up and down operating a donwhole pump. The tapered rod string is composed on different types of rods, composed of steel, fiberglass and other blended materials.

There are three main issues with rod pumps that decrease the efficiency of the system. Those are elasticity, viscous friction, and mechanical friction.

Because of the weight of the rods below and the fluid being lifted the rod string becomes elastic. This means that the heavy steel or fiberglass rod string will start acting like a giant spring. This elastic force takes the form of stress wave traveling up and down the rod string at the speed of sound. While the surface unit is seamlessly traveling up and down, parts of the rod string downhole are in tension while other parts are in compression.

Viscous friction is the viscous force imparted by the produced fluids on the outer diameter of the rod string resulting in continuous energy loss through the pumping cycle. Viscous friction is proportional to the velocity of the rod string.

Finally, mechanical friction occurs with the rod, couplings, guides, or pump come into contact with the tubing due to doglegs or pinch point created by deviation. Other forms of mechanical friction include paraffin, scale, and solids. Mechanical friction is directly related to wear and failures.

Because of elasticity and friction, the work done at the surface is not directly translated downhole. Energy is continuously lost to the system and reduces the efficiency of the entire installation.

In the case of mechanical friction, several solutions can be used to attenuate the effects of the mechanical friction over the entire system. One solution is to install rod guides, to be used in a sacrificial fashion and absorb the wear otherwise destined to wear the rods and coupling against the tubing. In this case, this essentially increases the friction of the system, increasing lifting costs. Another option is to decrease the friction in the well by applying coatings or installing thermoplastic liners. In this case, the rod string slides with much less friction against the tubing reducing the damage done to both.

Figure 1 shows a typical rod pump installation. In the next section, let's take a look at the balance of forces in a vertical well.

II) Vertical Model

a. Balance of Forces in a vertical wellbore

The forces acting on the rod string are displayed in Figure 2 and are composed of the buoyant weight of the rod element W , the tension force representing the upward pull on the rod element F_x , the tension force representing the pull from below on the rod element $F_{x+\Delta x}$, the damping force opposing the movement, F_d , resulting from fluid or viscous friction on the rod element's surface.

According to Newton's Second Law: "Conservation of Energy", we know that the sum of the forces exerted on an object are equal to the product of its mass times its acceleration:

$$\sum \vec{F} = m \cdot \vec{a},$$

where m is the mass of the object, \vec{a} its acceleration and \vec{F} the forces applied to the object. Therefore, the conservation of energy applied to the rod string gives:

$$\vec{F}_{x+\Delta x} - \vec{F}_x + \vec{W} - \vec{F}_d = m \cdot \vec{a}.$$

The weight, being a static force, can be dropped from the equation and reapplied after solution.

b. Elasticity term

In continuum mechanics, stress is a physical quantity which represents the internal forces exerted when one object applies a force to another. Stress, σ , results from a force, F , applied to an area, A , and is calculated using the following equation $\sigma = \frac{F}{A}$, hence its unit: pound per square inch.

The tension forces can be re-written using stress and area in a similar manner, such as:

$$F_x = S_x \cdot A,$$

$$F_{x+\Delta x} = S_{x+\Delta x} \cdot A,$$

Where S_x and $S_{x+\Delta x}$ are the rod stresses (psi) and A the cross-sectional area (in²).

Hooke's law is a law of physics that dictates the distance a spring will extend or compress when a force is applied to it, following the following equation: $F = k \cdot x$. In the previous equation F represents the force applied to the string, while k is the constant or stiffness of the string and x is the distance the spring extends or compresses.

Since rod stress are elastic and undergo elastic deformation, Hooke's law states that:

$$S = E \cdot \frac{\partial u}{\partial x},$$

Where E is Young's Modulus of Elasticity (psi) and $\frac{\partial u}{\partial x}$ is the rod strain or the change in rod displacement over the change in rod length.

Using the above equations, we get:

$$\vec{F}_{x+\Delta x} - \vec{F}_x = (S_{x+\Delta x} - S_x) \cdot A = E \cdot A \cdot \left(\frac{\partial u}{\partial x} \Big|_{x+\Delta x} - \frac{\partial u}{\partial x} \Big|_x \right) = E \cdot A \cdot \Delta x \cdot \frac{\partial^2 u}{\partial x^2}$$

c. Acceleration term

The acceleration force can be re-written as:

$$m \cdot a = \frac{\Delta x}{144} \cdot \frac{\rho A}{g} \cdot \frac{\partial^2 u}{\partial t^2}.$$

d. Damping term

The viscous damping force is proportional to the velocity and mass of the rod string such that:

$$F_d = c \cdot \frac{\Delta x}{144} \cdot \frac{\rho A}{g} \cdot \frac{\partial u}{\partial t},$$

Where c is the damping factor, ρ is the density of the rod material (lb/ft³), $g = 32.2$ is the gravitational constant.

The damping term of the wave equation stands for the irreversible energy losses that occur along the rod string from viscous forces only. The damping factor can be calculated using hydraulic horsepower, production, fluid specific gravity and fluid level using:

$$c = \frac{(550)(144g)(H_{PR} - H_{HYD})\tau^2 g}{\sqrt{2}\pi(\rho_i A_i L_i)S^2}$$

The above equation would work well if there was no deviation is present in the well and if the necessary quantities accurately reflected the well condition at the time of the stroke.

The damping factor can be initially calculated but can also be approximated through iteration, cf. [13].

e. The 1D-damped wave equation

Combining these above equations,

$$\vec{F}_{x+\Delta x} - \vec{F}_x + \vec{W} - \vec{F}_d = m \cdot \vec{a}$$

becomes

$$E \cdot A \cdot \Delta x \cdot \frac{\partial^2 u}{\partial x^2} - c \cdot \frac{\Delta x}{144} \cdot \frac{\rho A}{g} \cdot \frac{\partial u}{\partial t} = \frac{\Delta x}{144} \cdot \frac{\rho A}{g} \cdot \frac{\partial^2 u}{\partial t^2}$$

Replacing the velocity of sound of the rod material $v_s = \sqrt{\frac{144gE}{\rho}}$ in ft/s in the above and dividing by Δx gives:

$$v_s^2 \cdot \frac{\partial^2 u}{\partial x^2} - c \cdot \frac{\partial u}{\partial t} = \frac{\partial^2 u}{\partial t^2}$$

The above equation is the one-dimensional damped wave equation which models the propagation of stress waves in the rod string. As can be seen by the negative sign in the above equation, the damping factor is used to subtract energy to the wave equation to mimic the energy lost to viscous forces during the pumping operation. Therefore, the bigger the value of the damping factor the more energy is removed from the system resulting in a vertically skinnier card. While a low value of damping factor will have the opposite effect and result in a fatter looking downhole card.

The wave equation models friction of viscous origin only.

Also, it is important to note that in order to use the wave equation in the case of vertical wells, the assumption that there is no lateral movement of the rod string must hold. This means that we are assuming there is no contact between the rods, couplings, and the tubing, therefore, that there is no mechanical friction from deviated. In this case, the rod string can be compared to an ideal slender bar and the propagation of the stress waves becomes a one-dimensional phenomenon and the wave equation can be used to describe their propagation.

In the next section, two example solutions to the wave equation are presented.

III) Solutions to the vertical wave equation

a) The Gibbs method

Dr. Sam Gibbs commercialized his solution to the wave equation in 1967. Gibbs used complex theory and separation of variables to solve the wave equation by assuming a product solution:

$$z(x, t) = X(x)T(t),$$

And solving the following differential equations:

$$T''(t) + cT'(t) - \lambda_n^2 a^2 T(t) = 0,$$

$$X''(x) + \lambda_n^2 X(x) = 0.$$

The solution is given by:

$$u(x, t) = \frac{\sigma_0}{2EA}x + \frac{v_0}{2} + \sum_{n=1}^{\infty} O_n(x) \cos(n\omega t) + P_n(x) \sin(n\omega t)$$

For more information on the above, see [9].

Before Gibbs' solution, wells were exclusively controlled using surface data. Figure 3 shows a graph of the surface card for a stroke as well as the downhole cards at the top of each taper. Through this graph it is possible to see the progression from surface to downhole.

b) Finite difference solution

Finite differences are a mathematical technique that approximates the solution to differential equations by replacing derivative expressions with finite difference quotients. Those finite difference quotients transforms a complex problem into a linear equation ($\sim y = m \cdot x + b$) to be solved at every step down the rod string. This allows the capability of adapting to different taper properties.

$$\frac{\partial u}{\partial t} \approx \frac{u(x, t + \Delta t) - u(x, t)}{\Delta t}$$

$$\frac{\partial^2 u}{\partial t^2} \approx \frac{u(x, t + \Delta t) - u(x, t - \Delta t)}{\Delta t^2}$$

$$\frac{\partial^2 u}{\partial x^2} \approx \frac{u(x + \Delta x, t) - u(x - \Delta x, t)}{\Delta x^2}$$

One of the many advantages in using finite differences to solve the wave equation is the necessary creation of a mesh in both time and space. The rod string is discretized from surface to pump into M finite difference nodes, satisfying a stability condition. The time discretization is taken to be the points recorded at the surface data, i.e., the number of surface pairs of position and load. The space discretization is calculated to satisfy the stability conditions as detailed in [4].

This enables stress calculation at every finite difference node down the wellbore as opposed to at the top of every taper with the Gibb's solution. An example of a solution mesh is displayed in Figure 4.

As outlined in [3, 4, 11, 13], the solution becomes:

1) Using surface position data:

$$j = 1, \dots, N; u_{0,j} = Sfp_j,$$

2) Using Hooke's law and surface load data:

$$j = 1, \dots, N; u_{1,j} = \frac{Sfl_j \cdot \Delta x}{EA} + u_{0,j},$$

3) For $i = 2, \dots, M$:

$$u_{i+1,j} = \frac{1}{\left(\frac{EA}{\Delta x}\right)^+} \left\{ \left[\alpha(1 + c \cdot \Delta t) \right] \cdot u_{i,j+1} - \left[\alpha(2 + c\Delta t) - \left(\frac{EA}{\Delta x}\right)^+ - \left(\frac{EA}{\Delta x}\right)^- \right] \cdot u_{i,j} + \alpha \cdot u_{i,j-1} - \left(\frac{EA}{\Delta x}\right)^- \cdot u_{i-1,j} \right\}$$

The position and load data can be illustrated as a function of two variables and graphed to give surface and downhole dynamometer cards, as displayed in Figure 5.

So how good is the vertical model? In the next section, the Sandia experiment is presented, where downhole dynamometer tools were deployed in 6 vertical wells.

IV) Sandia

In the 1990's, the government contracted Sandia National Laboratory to conduct a series of tests to understand the high failure rates in rod pump applications. In 1986, Glenn Albert developed an electronic downhole dynamometer. Sandia commissioned a series of downhole dynamometer tools that were deployed in 6 vertical wells.

The Sandia National Laboratory compiled a series of test data collected with a set of five downhole tools built by Albert Engineering under contract to Sandia National. The memory tools were deployed in the sucker rod string and equipped with sensors that were capable of measuring pressure, temperature, load and acceleration.

Primarily, the motivation behind this research was to try to minimize sucker rod failures, which represented a significant cost to the oil industry. Up until the study, it was common practice to rely on load versus position information measured at the surface to infer stresses on the sucker rod string downhole, i.e., control using surface data.

For the Sandia wells, downhole data was calculated using the above-mentioned Gibbs' method. The calculated data was shown to be almost an exact match for the measured downhole data using the dynamometer tools. Sandia data validated the use of the wave equation to calculate downhole data.

This removed guess work from controlling rod pump wells. All the wells used for this study were vertical. Everything model in existence today with predictive or vertical is based on this data. Figure 6 and 7 show results of the measured Sandia data superimposed on calculated downhole data using the Gibbs' method and the Modified Everitt-Jennings methods, see [3, 11].

Downhole data is important because of the key control parameters it contains, such as net stroke, fluid load, friction, amount of gas in the downhole card. These quantities are essential for optimization and control and needed for the following calculations: inferred production, pump, and system efficiency, diagnose downhole conditions, fluid level calculation.

V) Deviated Case

In this section, axial loads in deviated wells are examined using the maximum load principle, where maximum pulling load is applied. During the upstroke, the highest tensile loading in the rod string is generated due to drag force and the coefficient of friction. The drag force magnitude depends on friction factor and the normal force exerted by the tubing.

Typical deviated hole has three major sections:

- Build – inclination increases with depth
- Drop – inclination decreases with depth
- Hold – constant inclination.

a) Build Section

In the build section, three different sections stand out, as depicted in Figure 9:

- Upper section: rod string is in contact with the upper part of the tubing with the normal force perpendicular to the direction of movement
- Middle section: rod string does not touch the sides of the tubing, contact force is zero
- Lower section: rod string rests on the bottom side of the tubing, normal force contributes to weight.

Figure 10 shows the normal force acting on a rod element in the build section.

Where F_x is the axial force, R is the radius of curvature, α is the inclination angle, F_n is the normal force.

From the Figure 10, we get:

$$\sin\left(\frac{|\Delta\alpha|}{2}\right) = \frac{\frac{1}{2}F_n}{F_x} = \frac{\text{opposite}}{\text{hypotenuse}},$$

$$\leftrightarrow F_n = 2 \cdot F_x \cdot \sin\left(\frac{|\Delta\alpha|}{2}\right).$$

Note that in this case the weight of the element and the normal force have opposite directions.

The forces applied to the rod string in the build section are displayed in Figure 11.

The resultant normal force is the vector sum of the normal components of the weight and axial force:

$$F_n = \Delta\alpha \cdot W \cdot R \cdot \sin \alpha - 2 \cdot F_x \cdot \sin\left(\frac{|\Delta\alpha|}{2}\right).$$

The magnitude of the associated drag force acting in a direction opposite the rod string movement is

$$F_{drag} = -c_f \cdot |F_n|.$$

The incremental force ΔF_x to pull the rod string element from rest is

$$\Delta F_x = |F_{drag}| - \Delta\alpha \cdot W \cdot R \cdot \cos \alpha.$$

At equilibrium we get

$$\frac{\partial F_x}{\partial \alpha} = -c_f \cdot \left| W \cdot R \cdot \sin \alpha - 2 \cdot F_x \cdot \sin\left(\frac{|\Delta\alpha|}{2}\right) \right| - W \cdot R \cdot \cos \alpha.$$

When in contact with the upper side of the tubing

$$\frac{\partial F_x}{\partial \alpha} = -c_f \cdot \left(2 \cdot F_x \cdot \sin\left(\frac{|\Delta\alpha|}{2}\right) - W \cdot R \cdot \sin \alpha \right) - W \cdot R \cdot \cos \alpha.$$

b) Drop Section

In the drop section, the rod string is in contact with the bottom part of the tubing with varied intensity throughout the entire section, see Figure 12.

In this case, the normal force is always positive and contributing to the weight force.

In the drop section of the wellbore, the normal force, weight, and axial force contribute to each other, as can be seen in Figure 13.

At equilibrium we get

$$\frac{\partial F_x}{\partial \alpha} = c_f \cdot \left(W \cdot R \cdot \sin \alpha + 2 \cdot F_x \cdot \sin \left(\frac{|\Delta \alpha|}{2} \right) \right) + W \cdot R \cdot \cos \alpha.$$

c) Hold Section

In the hold section of the wellbore, the tensional load depends only on the direction of the stroke, as can be seen in Figure 14.

The balance of forces reads:

$$\frac{\partial F_x}{\partial x} = W \cdot (c_f \cdot \sin \alpha + \cos \alpha).$$

During the upstroke, while pulling out of the hole, the tensional load equals:

$$F_x + \Delta x = F_x + W \cdot (MD_1 - MD_2) \cdot (c_f \cdot \sin \alpha_1 + \cos \alpha_1).$$

During the downstroke – running in the hole, the tensional load equals:

$$F_x + \Delta x = F_x + W \cdot (MD_1 - MD_2) \cdot (\cos \alpha_1 - c_f \cdot \sin \alpha_1).$$

Looking at the above equations, the problem seems well within our reach. However, all the above equation are 2-dimensional only. This means that for all the above cases, the azimuth angle is assumed to be zero. Both azimuth and inclination change simultaneously creating a phenomenon called tortuosity.

Figure 14 depicts a well bore showing the tortuosity and inclination changes over the path of the trajectory.

VI) Solutions to the deviated problem

a) The Gibb's deviated method

To address the deviated model, Gibbs presented a modified form of the wave equation:

$$\frac{\partial^2 u(s, t)}{\partial t^2} = v^2 \frac{\partial^2 u(s, t)}{\partial s^2} - c \frac{\partial u(s, t)}{\partial t} - C(s) + g(s),$$

And

$$C(s) = \frac{\partial u(s, t) / \partial t}{|\partial u(s, t) / \partial t|} \cdot \mu(s) \left[Q(s) + T(s) \cdot \frac{\partial u(s, t)}{\partial s} \right].$$

Where $C(s)$ represents the Coulombs friction force and $g(s)$ represents the rod weight term in the non-vertical case. This method is outlined in [8].

b) Lukasiewicz method

Lukasiewicz approach involves solving a system of coupled fourth order nonlinear differential equations by analyzing the problem separately in both the axial and transverse direction, as described in [10, 12].

In the axial direction, the problem becomes:

$$\frac{\partial F}{\partial s} - \gamma \cdot A \frac{\partial^2 u}{\partial t^2} + \gamma \cdot g \cdot A \cdot \cos \theta - D \cdot \frac{\partial u}{\partial t} - F_t = 0,$$

And in the transverse direction:

$$EI \cdot \frac{\partial}{\partial s^2} \left[\frac{\partial^2 v}{\partial s^2} + \frac{1}{R_\phi} \right] + \gamma \cdot A \frac{\partial^2 v}{\partial t^2} + n_t + n_p + D_t \cdot \frac{\partial v}{\partial t} + \frac{F}{R} - \gamma \cdot g \cdot A \cdot \sin \theta = 0.$$

The Gibbs method has been successfully used in the predictive case for many years. There are several other methods for solving the deviated problem published in the industry today, this paper only focuses on the above two.

c) Horizontal Well Deviated Downhole Data Acquisition (HWDDDA)

As described in the above section, wells were controlled from surface data before data from the Sandia experiment surfaced, which validated the use of the wave equation for the calculation of downhole data in vertical wells.

The majority of the methods and models available in the industry today are based on the Sandia's vertical data. This explains why the deviated predictive models are inaccurate. As discussed in the previous section, the deviated problem is very complex and so far has only been solved by making assumptions.

For instance, a common assumption, which simplifies the deviated problem by several orders of magnitude is that the rod string lies on the tubing in its entire length. We know that not to be true. The rod string only comes in contact with the tubing at points where it bends, buckles, or at the rod guides and couplings. What happens to the dynamics of the rod string in between those points?

In an effort to bring clarity to this problem and reduce the number of rod pump failures due to deviation as well as help the industry come up with better solutions, the Artificial Lift Research and Development Council (ALRDC) provide the seed money to start the Horizontal Well Deviated Downhole Dynamometer Acquisition (HWDDDA) project. The goal of this project is to directly measure load and position data, required to validate and improve the accuracy of the existing software for deviated wells.

This involves designing and building downhole dynamometer tools and deploying those tools in deviated & horizontal wells.

Figure 16 shows a schematic of the downhole tool.

Multiple tools will be deployed throughout the rod string at strategic location with respect to the deviation survey so that the maximum impact of the deviated nature of the well and its effect on the rod string can be captured by the acquired data. To measure the effects of bending, tools for example will be placed before and after a dog leg. Another tool will be located at the pump.

The synchronized tools will capture data according to an acquisition schedule including valve tests. The tools will then be retrieved, and the data downloaded. After the data is validated, it will be made first accessible to the members of the project and then to the industry similar to the Sandia data. Any company interested in participating in this project, particularly to contribute wells for testing should contact the author of this paper.

Participants in the project will have first access to data, results, and developed tools.

CONCLUSIONS

There are vast differences between vertical and deviated application of the rod pumping. The majority of the methods and models available today are based on the vertical data collected during the Sandia experiment.

Several essential points should be taken away from this presentation. The first, is that the practice of drilling should be controlled more rigorously so that the deviation and tortuosity is kept to a minimum. Most drilling crews are under tight restraint from management and investors to drill a well as quickly as possible with little regard to how difficult the well will be pumped afterwards.

Rod pumping in vertical wells is very well understood and does not present a problem in operation. The deviated case, however, is still not well understood and as described above, very difficult to manage. Current available deviated predictive models have shortcomings and do not describe the dynamics of the rod string accurately, which causes problem for the operators down the line. Similarly, the deviated diagnostics available today either introduce anomalies in the data or are ineffective with shallow deviation.

In order to be more efficient in dealing with deviation in rod pump wells, more data is needed to both validate and create better models.

REFERENCES

1. Bommer, P.M. and Podio, A.L.: "Beam Lift Handbook." The University of Texas at Austin Petroleum Extension, 2015.
2. Ehimeakhe, V.: "Calculating Pump Fillage for Well Control using Transfer Point Location", SPE Eastern Regional Meeting, 12-14 October 2010, Morgantown, West Virginia, USA.
3. Ehimeakhe, V.: "Comparative Study of Downhole Cards Using Modified Everitt-Jennings Method and Gibbs Method", Southwestern Petroleum Short Course 2010.
4. Everitt, T. A. and Jennings, J. W.: "An Improved Finite-Difference Calculation of Downhole Dynamometer Cards for Sucker-Rod Pumps," paper SPE 18189 presented at the 63rd Annual Technical Conference and Exhibition, 1988.
5. Gibbs S. G., "Rod Pumping: Modern Methods of Design, Diagnosis and Surveillance", 2012
6. Gibbs, S. G., and Neely, A. B.: "Computer Diagnosis of Down-Hole Conditions in Sucker Rod Pumping Wells," JPT (Jan. 1996) 91-98; *Trans.*, AIME, 237
7. Gibbs, S. G.: "A Review of Methods for Design and Analysis of Rod Pumping Installations," SPE 9980 presented at the 1982 SPE International Petroleum Exhibition and Technical Symposium, Beijing, March 18-26.
8. Gibbs, S. G.: "Design and Diagnosis of Deviated Rod-Pumped Wells", SPE Annual Technical Conference and Exhibition, Oct 6-9, 1991, Dallas, USA.
9. Gibbs, S.G.: "Method of Determining Sucker-Rod Pump Performance," U.S. Patent No. 3,343,409 (Sept. 26, 1967).
10. Lukasiewicz, S. A.: "Dynamic Behavior of the Sucker Rod String in the Inclined Well", Production Operations Symposium, April 7-9, 1991, Oklahoma City, Oklahoma, USA.
11. Pons, V.: "Modified Everitt-Jennings: A complete Methodology for Production Optimization of Sucker Rod Pumped Wells.", Southwestern Petroleum Short Course 2015, Lubbock, TX.
12. Pons-Ehimeakhe, V.: "Implementing Coulombs Friction For The Calculation of Downhole Cards in Deviated Wells.", 2012 SouthWestern Petroleum Short Course, Lubbock TX, April 17-18th.
13. Pons-Ehimeakhe, V.: "Modified Everitt-Jennings Algorithm with Dual Iteration on the Damping Factors.", 2012 SouthWestern Petroleum Short Course, Lubbock TX, April 17-18th.
14. Schafer, D. J. and Jennings, J. W.: "An Investigation of Analytical and Numerical Sucker-Rod Pumping Mathematical Models," paper SPE 16919 presented at the 1987 SPE Annual Technical Conference and Exhibition, Dallas, Sept. 27-30.
15. Snyder, W. E.: "A Method for Computing Down-Hole Forces and Displacements in Oil Wells Pumped with Sucker Rods," paper 851-37-K presented at the 1963 Spring Meeting of the API Mid-Continent District Div. of Production, Amarillo, March 27-29.
16. Takács, G.: "Sucker-Rod Pumping Manual." PennWell, 2002.
17. Waggoner, J. R.: "Insights from Downhole Dynamometer Database", Southwestern Petroleum Short Course -97.

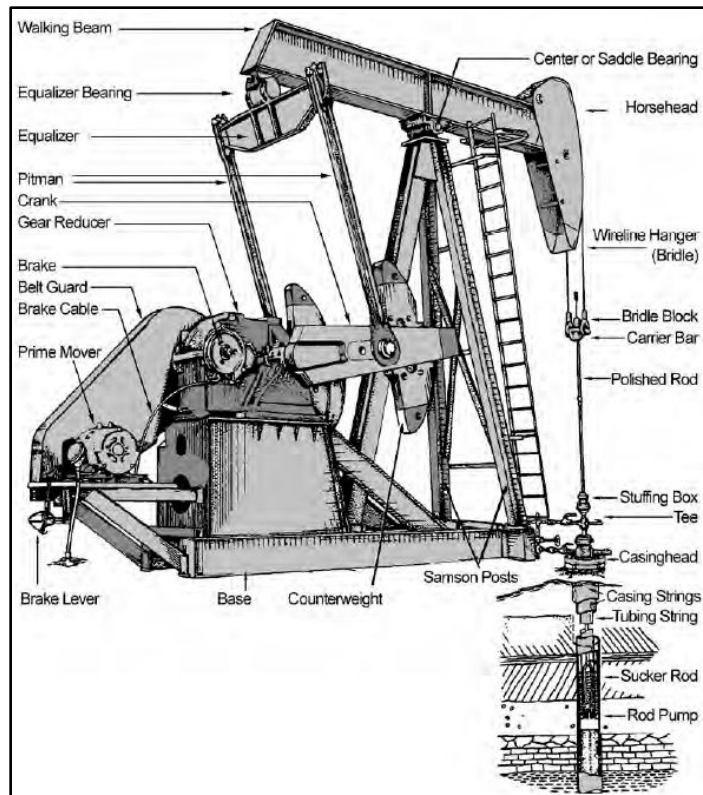


Figure 1: Pumping Unit installation.

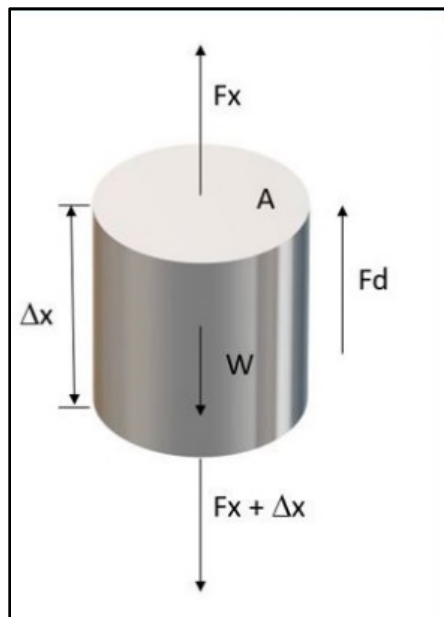


Figure 2: Forces acting on rod element in a vertical well.

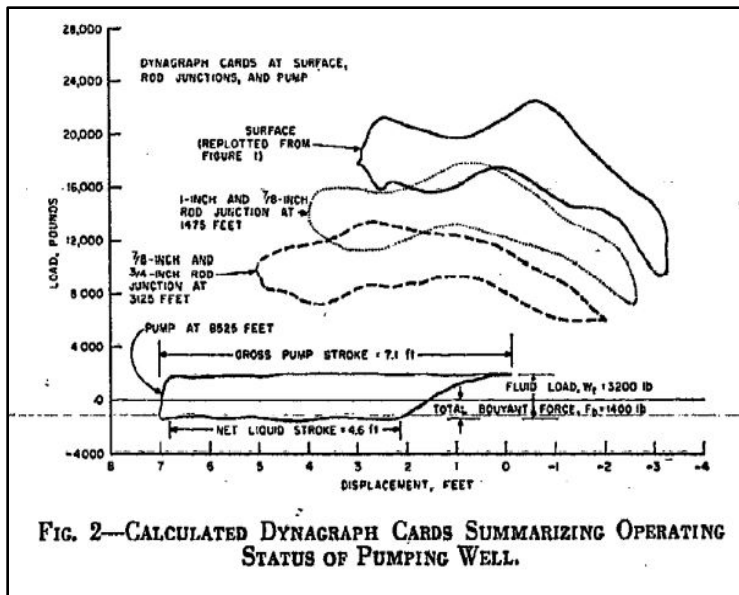


Figure 3: "Computer Diagnosis of Down-Hole Conditions in Sucker Rod Pumping Wells", S.G. Gibbs, A.B. Neely, Journal of Petroleum Technology, January 1966

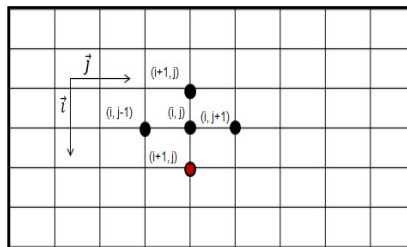


Figure 4: Illustration of finite difference mesh.

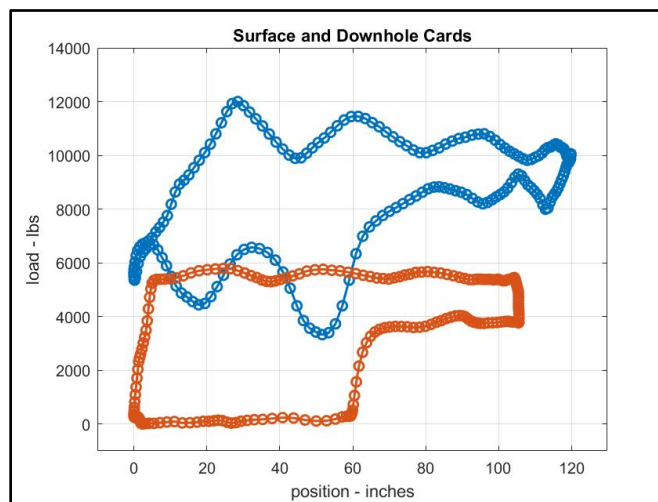


Figure 5: Picture of Surface and Downhole card.

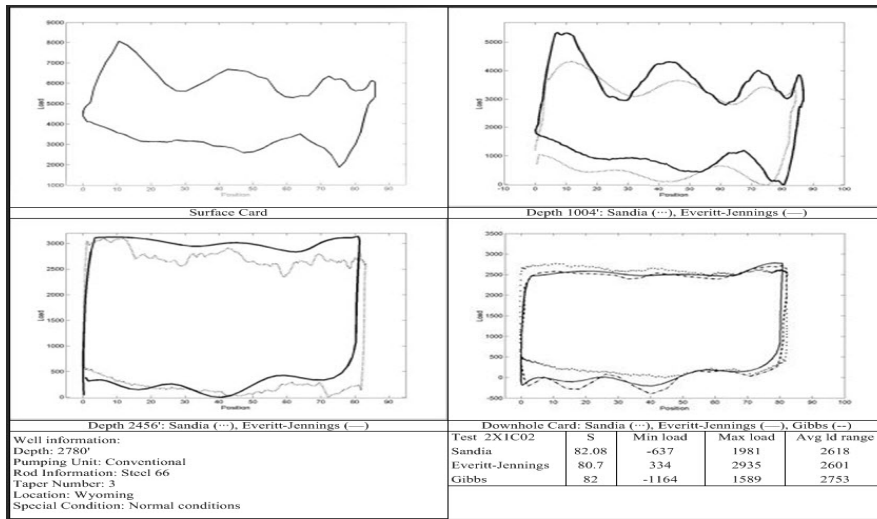


Figure 6: Comparison of measured Sandia data with calculated donwhole data using the Gibbs' method and the modified Everitt-Jennings method on a conventional well.

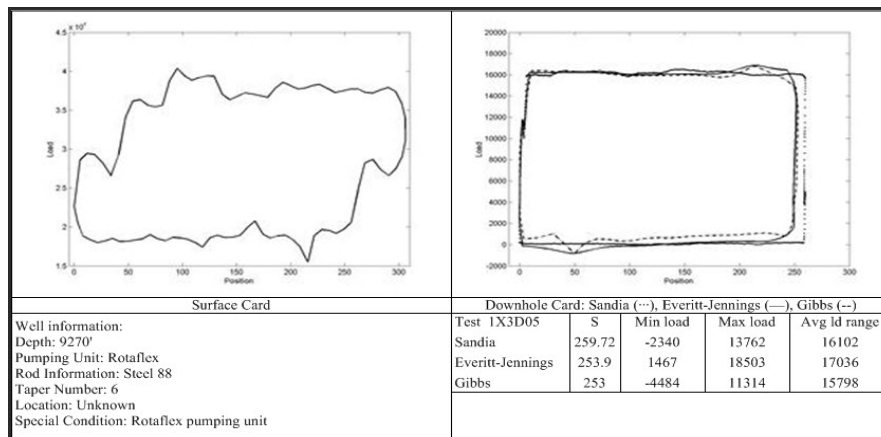


Figure 7: Comparison of measured Sandia data with calculated donwhole data using the Gibbs' method and the modified Everitt-Jennings method on a conventional well.

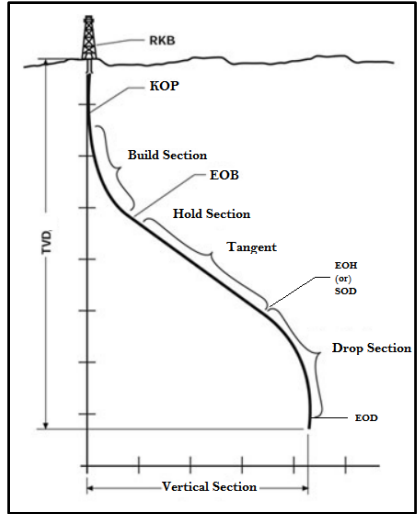


Figure 8: Picture of a deviated wellbore showing build, hold and drop section.

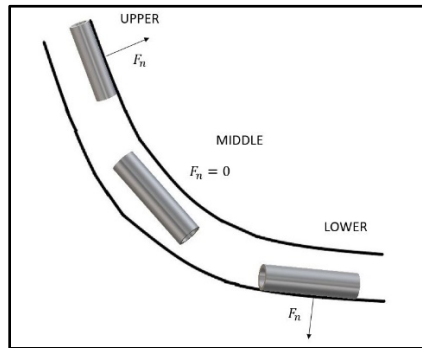


Figure 9: Picture of build section containing upper, middle, and lower section.

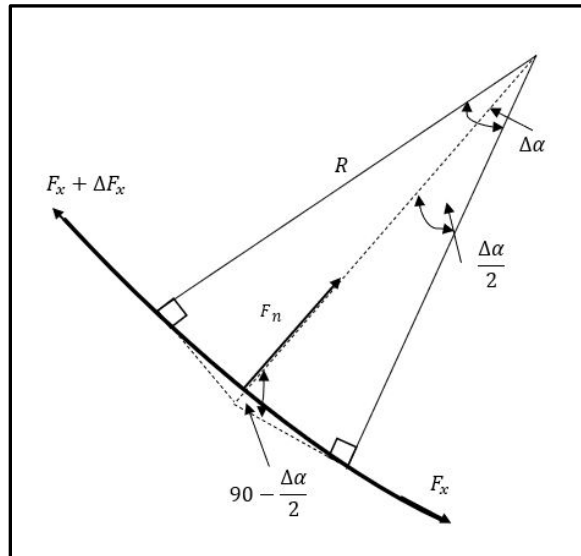


Figure 10: Normal force in the case of the build section.

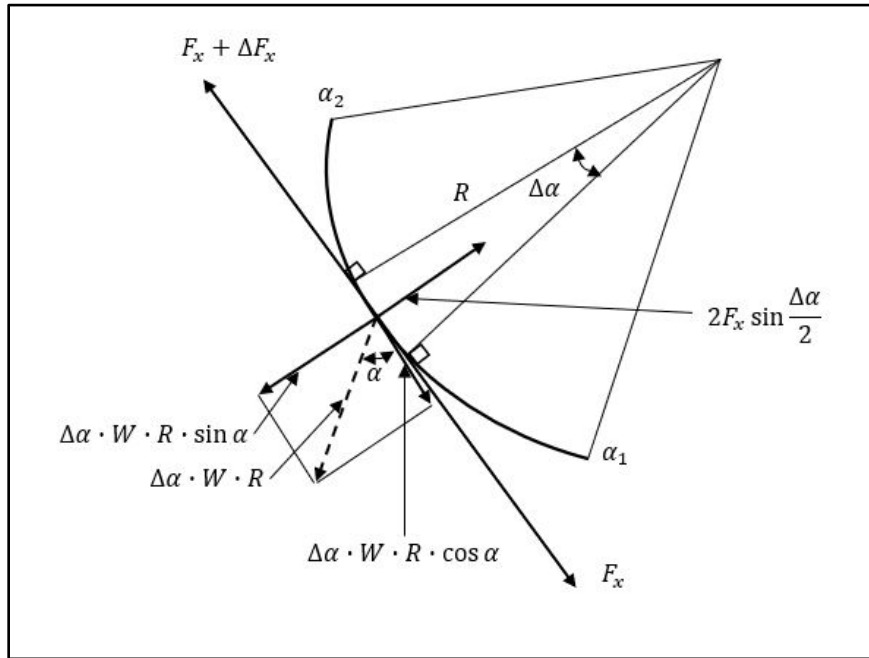


Figure 11: Forces acting on a rod element in a deviated wellbore – build section.

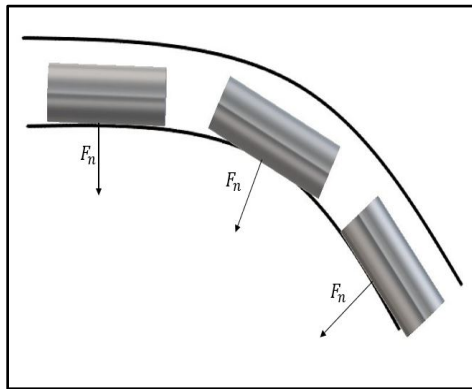


Figure 12: Picture of the drop section of a deviated wellbore.

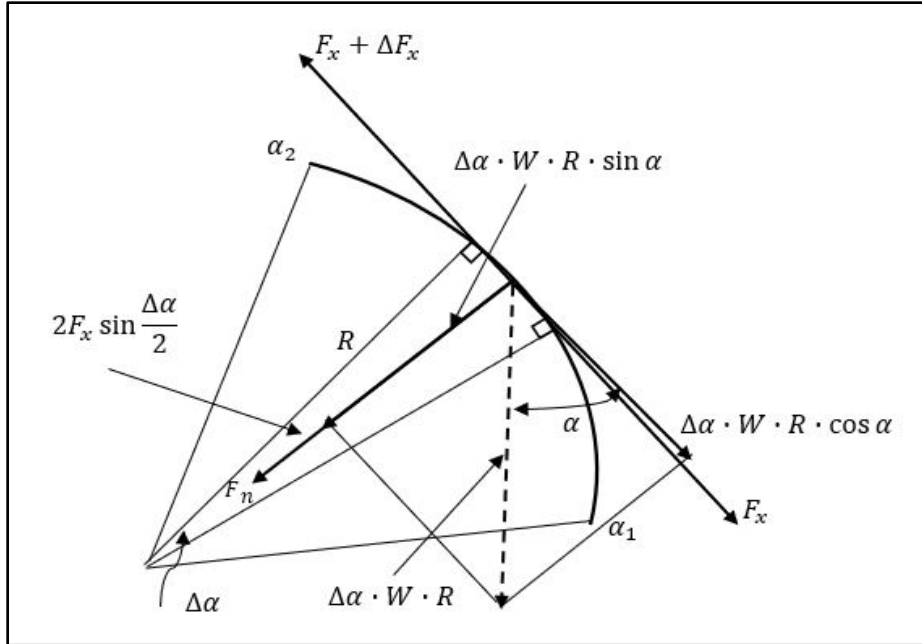


Figure 13: Forces acting on a rod element in the drop section of a deviated wellbore.

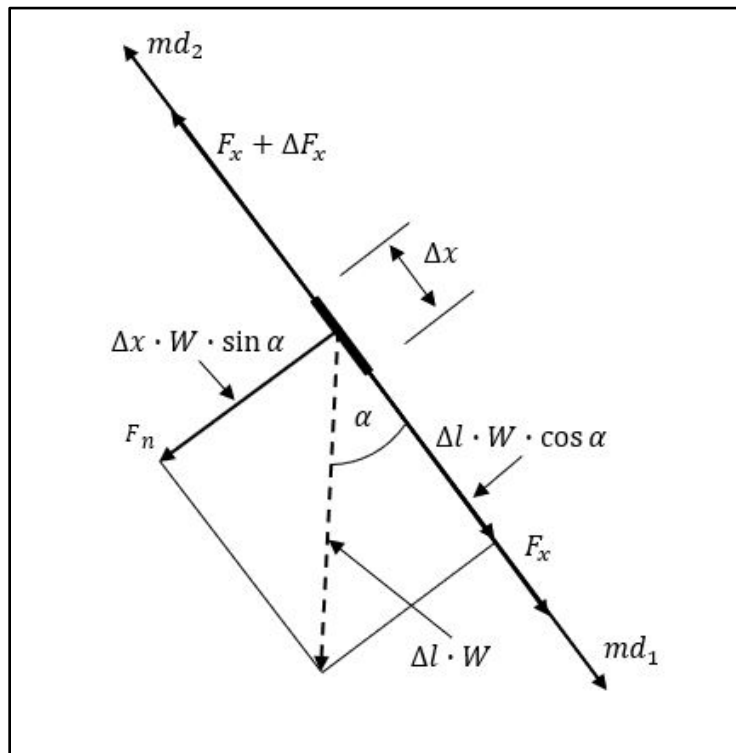


Figure 14: Forces acting on a rod element in the hold section of a deviated wellbore.

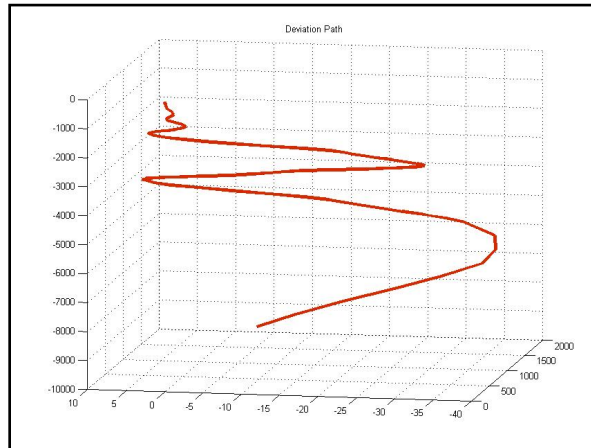


Figure 15: Example of inclination and tortuosity in a deviated well.

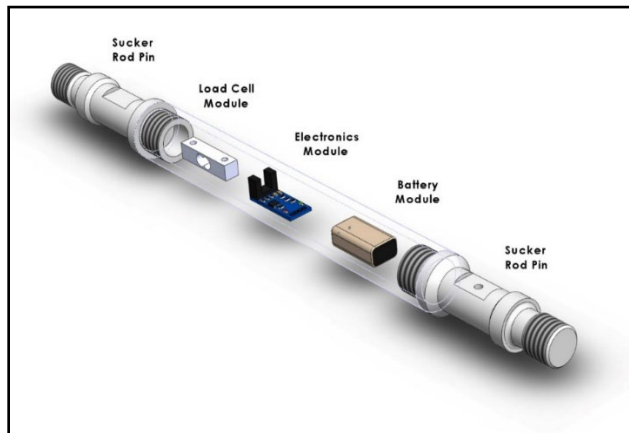


Figure 16: Schematics of downhole load cell tool for HWDDDA project.